EQUATION-BASED MODEL FOR SIMULTANEOUS WORKING FLUID - PROCESS - HEAT INTEGRATION OPTIMIZATION OF ORGANIC RANKINE CYCLE FOR LIQUEFIED NATURAL GAS REGASIFICATION

Yingzong Liang[1]*, Zhi Yang[1], Jianyong Chen[1], Xianglong Luo[1], Ying Chen[1]

[1]School of Materials and Energy, Guangdong University of Technology,
Guangzhou, China
yliang@gdut.edu.cn

* Corresponding Author

ABSTRACT

In this paper, an equation-based model is developed for the simultaneous process-working fluid-heat integration optimization of LNG regasification process using ORC for cold energy recovery. We integrate a rigorous thermodynamics module based on SRK equation of state in our model to ensure an accurate computation of thermodynamic properties (e.g. vapor-liquid equilibrium and enthalpy) so that the composition of the working fluid can be optimized. To address the computational difficulties, we introduce an efficient formulation approach for heat integration that significantly reduces binary variables compared with conventional formulation. Thanks to the efficient formulation and rigorous thermodynamic calculation, our model is capable of solving the simultaneous optimization problem effectively. We apply our model to a LNG-ORC process design problem to demonstrate its efficiency.

1. INTRODUCTION

The organic Rankine cycle (ORC) has been identified as a promising technology to harvest electric energy from low-grade heat sources (Chu and Majumdar, 2012). Intrinsically, the energy conversion efficiency of ORC is governed by the temperature ratio between its heat sink and heat source. Often, the temperature of low-grade heat sources is below 373 K, which limits the efficiency of the ORC operating with typical heat sinks (e.g. air and water) at about 300 K. Therefore, choosing a suitable heat sink at a lower temperature can bring substantial improvement to the energy efficiency.

Among different options, liquefied natural gas (LNG) is an excellent heat sink for its cryogenic temperature (~120 K) and massive heat absorption during regasification. However, studies show that over 95% of current regasification processes simply warm up LNG by seawater using open rack vaporizers, resulting in an enormous cold energy loss (Park et al., 2019). As LNG is projected to meet 8% of the global energy demand in 2050 (ExxonMobil, 2018, U.S. Energy Information Administration, 2017), there is a tremendous economic potential to recover LNG cold energy by integrating the ORC and regasification processes.

Increasing attention has been paid to the design of ORC for LNG cold energy recovery. Comprehensive review can be found in Kanbur et al. (2017). Economic research has demonstrated the integrated ORC-LNG regasification process is more profitable than the open rack vaporizer (Park et al., 2019). Numerous computational studies have shown considerable improvements in energy efficiency of the processes by optimizing their design, heat integration, and working fluid composition. Often, operating temperatures, pressures, and stream flow rates are varied to search for the best design that achieves the highest power output (Lee, S., 2017). Besides operating parameters, working fluid composition has a significant impact on the ORC performance. In general, mixed working fluids outperform the pure ones for their variable evaporating temperatures that their heat profiles have a better match to the ones of heat source/sink, and subsequently reduce system's exergy loss. Luo et al. (2019) tackled the working

fluid design problem by developing an artificial neural network-group contribution method that accurately estimates the fluid properties, along with a procedure to evaluate the performance of the working fluid. Further, due to the dramatically change of heat capacity during phase change and the variable stream properties (e.g. temperature and heat capacity) as a result of process and working fluid optimization, simultaneous process-heat integration optimization method is required to carry out heat integration with variable stream data.

Previous studies are mostly based on a sequential scheme that performs working fluid selection, process design, and heat integration optimization in a step-wise manner. This method, although intuitive, usually leads to suboptimal design since it neglects the tradeoffs among the steps. On the other hand, equation-based approach has a significant advantage over the sequential method that it is able to simultaneously optimize the working fluid, process design, and heat integration of the ORC. However, numerical difficulties remain for the equation-based method since the model needs rigorous thermodynamic calculation to obtain physical properties of the working fluid. Further exacerbating the problem is the conventional heat integration modeling approaches, which include many binary variables, and thus dampen the computational efficiency. Therefore, efficient modeling and optimization methods are necessary.

In this paper, we propose an equation-based mixed-integer nonlinear programming (MINLP) model to achieve simultaneous optimization of the ORC-LNG process. The model takes process design, working fluid composition, and heat integration into account, and determines their best combination to maximize the net power output. For the thermodynamic calculation, Soave-Redlich-Kwang (SRK) equation of state (Soave, 1972) is embedded to estimate stream properties, e.g. vapor-liquid equilibrium and enthalpy. In terms of the heat integration, we introduce an efficient modeling method (Hui, 2014) to reduce the number of binary variables.

Novelty of this paper is summarized as follows.

- We simultaneously optimize working fluid, process design, and heat integration of the ORC-LNG process.
- Accurate physical property calculation is accomplished thanks to the encoded thermodynamic constraints inside the equation-based model.
- The number of binary variables is greatly reduced by applying a computationally efficient and rigorous heat integration modeling method.

In following sections, we start by developing an equation-based model that considers thermodynamics, process design, and heat integration of the ORC-LNG process. We then apply the model to optimize the process to determine the best process design, working fluid composition, and heat integration that achieve the highest power output. Finally, we summarize the paper in section 5.

2. PROBLEM STATEMENT

2.1 Process Description

In this paper, we use a simple ORC (Figure 1) to illustrate the proposed model. Here the LNG stream (s_{lng}) is compressed to its transmission pressure, then vaporizes by exchanging heat with the working fluid leaving the turbine ($TURB$). For the working fluid, after condensing into liquid in the condenser ($COND$), it is compressed by the working fluid pump ($PUMPWF$) to a higher pressure, then heated up by seawater and vaporizes in $EVAP$. The gaseous state working fluid is sent to the turbine for expansion, of which the work is converted into electric energy. Specifications of the process are listed in **Table 1**.

2.2 Major Assumptions

Major assumptions of the model are summarized as follows.

- Flow rates, temperatures, pressures, and composition of the LNG streams are fixed.
- Inlet and outlet temperatures of seawater are fixed, and its heat capacity flow rate is a variable.

- The mixed working fluid consists of four components: CH_4, C_2H_6, C_3H_8, n-C_4H_{10}, which are also the alkane substances in natural gas for their suitable boiling point temperatures, availability, and safety. The flow rate and composition of working fluid are to be optimized.
- The working fluid compression and expansion processes are isentropic with efficiencies of 0.7 and 0.8, respectively.
- The evaporator ($EVAP$) is assumed as a simple heater using seawater as heat source, which is at 293.15 K and warms up the working fluid to 283.15 K.

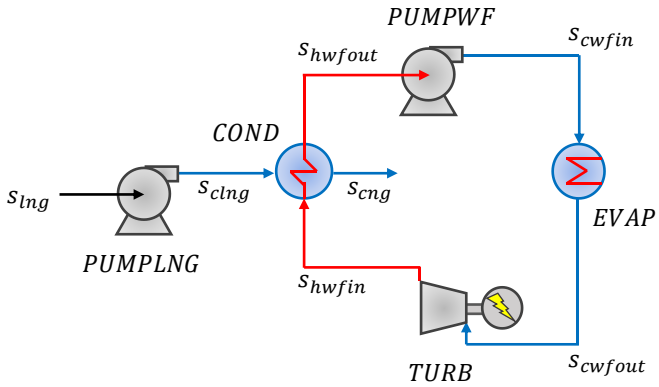

Figure 1: Process flowsheet of the simple ORC utilizing LNG cold energy for power generation

Table 1: Specifications of the ORC

Specifications		**LNG Composition (mol/mol LNG)**	
Outlet temperature working fluid at $EVAP$ (K)	283.15	N_2	0.028
Outlet pressure of $PUMPWF$ (bar)	≤ 20	CH_4	0.898
Outlet pressure of $TURB$ (bar)	≥ 1.013	C_2H_6	0.055
Inlet temperature LNG (K)	123.46	C_3H_8	0.018
Inlet pressure LNG (bar)	30	n-C_4H_{10}	0.001
Flow rate of LNG (mol/s)	1		
Minimum approach temperature of $COND$ (K)	2		

3. MODEL FORMULATION

3.1 Modeling Framework

We propose an equation-based MINLP model for simultaneous optimization of the process design, working fluid composition, and heat integration of the ORC-LNG process. The model takes a form of **(M1)**.

(M1)

max $power$
s.t.
Process and equipment constraints
Heat exchangers constraints
Thermodynamic constraints

The objective of the model is to maximize power output of the ORC. The constraints can be classified into three categories, and in this paper, we only detail the objective function and some of the constraints.

- The process constraints to represent the connection of streams and equipment, and equipment constraints (except heat exchangers) to simulate its performance, and mass and energy balance.
- The heat exchanger constraints, which is able to handle variable stream properties (e.g. temperature and heat capacity flow rate), to guarantee feasible heat transfer among process streams.
- Thermodynamic constraints for streams' thermodynamic properties calculation (e.g. enthalpy and vapor-liquid equilibrium).

3.2 Objective Function

The objective of the model is to maximize the power output of the ORC, which is calculated by Eq. (1).

$$power = -\sum_{e \in EMEC} w_e \tag{1}$$

where e is the index of equipment, $EMEC$ is the set of equipment what consumes electric energy, and w_e is the electric power input (positive) or output (negative) of equipment.

3.3 Process and Equipment Constraints

Mass balance of equipment is expressed as Eq. (2) that each substance's molar flow rate of inlet streams is equal to the one of outlet streams.

$$f_{s,u}^{com} = f_{s',u}^{com} \quad (e,s,s') \in EQSP, (s,u), (s',u) \in SU \tag{2}$$

where s is the index of stream, u is the index of substance, $EQSP$ is he set of inlet (s) and outlet (s') streams pairs of equipment (e), SU is the set of substance (u) in stream (s), and $f_{s,u}^{com}$ is molar flow rates.

Eq. (3) is the energy balance of the turbine and working fluid pump, and Eq. (4) represents the isentropic expansion of process streams in the turbine.

$$w_e = h_{s'} - h_s \quad (e,s,s') \in TURBSP \cup PUMPSP \tag{3}$$

$$1000(mh_{s'} - mh_s) = \eta_e \frac{z_s \cdot R \cdot t_s}{\frac{\gamma - 1}{\gamma}} \left[\left(\frac{p_{s'}}{p_s} \right)^{\frac{\gamma-1}{\gamma}} - 1 \right] \quad (e,s,s') \in TURBSP \tag{4}$$

where $TURBSP$ and $PUMPSP$ are respectively the sets of inlet and outlet streams pairs of turbine and pump, h_s is stream enthalpy, mh_s is molar enthalpy, z_s is a compressibility factor, t_s is stream temperature, p_s is stream pressure, η_e is isentropic efficiency, and γ denotes specific heat ratio.

3.4 Heat Exchanger Constraints

Eqs. (5)-(8) describe the performance of the heat exchanger ($COND$) that it guarantees energy balance and feasible heat transfer between hot and cold streams. Eq. (5) represents the overall heat balance of the heat exchanger, Eqs. (6)-(7) calculate enthalpy change of streams, Eq. (8) ensures that the heat surplus above all pinch candidates (s'') must be nonnegative.

$$\sum_{(s,s') \in EXSP} q_{e,s,s'} = 0 \quad e \in EX \tag{5}$$

$$q_{e,s,s'} = fcp_s(t_s - t_{s'}) \quad (e,s,s') \in EXSP \tag{6}$$

$$q_{e,s,s'} = h_s - h_{s'} \quad (e,s,s') \in EXSP \tag{7}$$

$$\sum_{(s,s') \in EXSP} qa_{e,s,s',s''} \geq 0 \quad (e,s'') \in EXIN \tag{8}$$

where EX is the set of heat exchangers, $EXSP$ is the set of inlet and outlet streams pairs of heat exchangers, $EXIN$ is the set of inlet stream of heat exchangers, $q_{e,s,s'}$ is enthalpy change of the inlet (s) and outlet (s') streams of heat exchanger (e), fcp_s is heat capacity flow rate, $qa_{e,s,s',s''}$ represents stream enthalpy change above pinch candidate (s''), and detailed calculation of $qa_{e,s,s',s''}$ can be found in Hui (2014). Major advantages of Hui's formulation is that it only requires half of the binary variables of traditional approaches, and thus is more computationally efficient.

3.5 Thermodynamic Constraints

Thermodynamic constraints is developed based on the SRK equation of state (Eq. (9)).

$$z_s^3 - z_s^2 + \left[a_s^{cap} - b_s^{cap} - \left(b_s^{cap} \right)^2 \right] z_s - a_s^{cap} \cdot b_s^{cap} = 0 \quad s \in SSTATEUK \tag{9}$$

$$3z_s^2 - 2z_s + a_s^{cap} - b_s^{cap} - \left(b_s^{cap}\right)^2 \geq 0 \quad s \in SSTATEUK \tag{10}$$

$$z_s - \frac{1}{3}\left(1 + b_{s'}^{cap} - b_{s'}^{cap}\right) \geq 0 \quad s \in SSTATEUK \cap SV \tag{11}$$

$$z_s - \frac{1}{3}\left(1 + b_{s'}^{cap} - b_{s'}^{cap}\right) \leq 0 \quad s \in SSTATEUK \cap SL \tag{12}$$

where $SSTATEUK$ is the set of streams that their states (i.e. temperature, pressure, or composition) are unknown, SV and SL are respectively the sets of vapor and liquid streams, a_s^{cap} and b_s^{cap} are dimensionless coefficients related to the composition, temperature, and pressure of process streams. Since Eq. (9) is a cubic equation, it may have three real roots (vapor, middle, and liquid) of which only one represents the true state of a stream, and the model may obtain one of the other two incorrect roots. To tackle this issue, we apply Eqs. (10)-(12) proposed by Kamath et al. (2010) to guarantee the model only converges on the correct root. Here, the LHS of Eq. (10) is the first derivative of the SRK equation to enforce its root to be either vapor root or liquid root, and the LHS of Eqs. (11) and (12) are the second derivatives of the SRK equation. Eq. (11) ensures the root to be a vapor, and Eq. (12) be a liquid.

Vapor-liquid equilibrium is governed by Eq. (13) that the fugacity of liquid (LHS) is equal to that of vapor (RHS) at equilibrium.

$$x_{s',u}^{com} \cdot \varphi_{s',u} = x_{s'',u}^{com} \cdot \varphi_{s'',u} \quad (s,s') \in SSL, (s,s'') \in SSV, s' \in SSTATEUK, s'' \in SSTATEUK, (s,u) \in SU \tag{13}$$

$$ln\left(\varphi_{s,u}\right) = b'^{cap}_{s,u}(z_s - 1) - ln\left(z_s - b_s^{cap}\right) - \frac{a_s^{cap}}{b_s^{cap}}\left(a'^{cap}_{s,u} - b'^{cap}_{s,u}\right) ln\left(1 + \frac{b_s^{cap}}{z_s}\right) \quad (s',s) \in SSL \cup SSV, s \in SSTATEUK, (s',u) \in SU \tag{14}$$

where SSL and SSV are respectively the sets of vapor (s') and liquid (s'') sub-streams of the mixed stream (s), $x_{s,u}^{com}$ is mole fraction, and $\varphi_{s,u}$ is fugacity coefficient calculated by Eq. (14), $a'^{cap}_{s,u}$ and $b'^{cap}_{s,u}$ are dimensionless coefficient related to temperature, pressure, and composition of process stream.

Molar enthalpy is a summation of ideal gas enthalpy (mh_s^0) and enthalpy departure (Δmh_s^{depart}) as presented in Eq. (16).

$$h_s = f_s \cdot mh_s \quad s \in STATEUK \tag{15}$$

$$mh_s = mh_s^0 + \Delta mh_s^{depart} \quad s \in STATEUK \tag{16}$$

where mh_s^0 is calculated by a simple mixing rule in Eq. (17), and Δmh_s^{depart} is given by Eq. (18).

$$mh_s^0 = \sum_{u \in SU}\left[x_{s,u}^{com}\int_{T^{ref}}^{t_s} cpig_u(t)dt\right] \quad s \in STATEUK \tag{17}$$

$$\Delta mh_s^{depart} = \left(a_s - t_s\frac{\partial a_s}{\partial t_s}\right)\frac{1}{b_s}\ln\left(\frac{z_s}{z_s + b_s^{cap}}\right) + R \cdot t_s(z_s - 1) \quad s \in STATEUK \tag{18}$$

$$\int_{T^{ref}}^{t_s} cpig_u(t)dt = \frac{A_u^{CPIG}}{3}\left[t_s^3 - \left(T^{ref}\right)^3\right] + \frac{B_u^{CPIG}}{2}\left[t_s^2 - \left(T^{ref}\right)^2\right] + C_u^{CPIG}\left(t_s - T^{ref}\right) \quad s \in STATEUK, (s,u) \in SU \tag{19}$$

where $cpig_u(t)$ is a polynomial function to compute ideal gas heat capacity (Eq. (19)), a_s is a correction factor related to temperature, pressure, and composition of process streams, and T^{ref} is reference temperature.

4. RESULTS AND DISCUSSION

Here we apply our model to optimize the working fluid composition, process design, and heat integration of the ORC-LNG process (**Figure 1**). Efficiencies of the turbine and pump are assumed to be 0.8 and 0.7 (Liu and Guo, 2011). The model is implemented on GAMS 24.7.4 (Brooke et al., 2003) and solved by SBB (Bussieck and Drud, 2001). The calculation is performed on an Intel i7-8700 CPU @ 3.20 GHz desktop PC with 8 GB RAM, and only one core is used for computation. The model has

3319 variables and 4238 constraints, and is solved in 54.5 CPU seconds. We verify our solution by Aspen Plus simulation.

Figure 2 verifies the GAMS results by comparing flash calculation results of s_{cwfout} to the simulation, which is carried out at 1375 kPa (the optimal solution) for a temperature range from 235-249 K (two-phase region). **Figure 2**(a) demonstrates that the compressibility factors computed by GAMS are almost identical to the ones of Aspen Plus. Here, the errors of vapor compressibility factors are less than ±0.1%, and the errors of the liquid ones are less than ±0.3%. **Figure 2**(b) and (c) respectively show the change of the stream's vapor fraction and mole fraction of components in vapor phase in terms of temperature change. **Figure 2**(d) compares the enthalpy change calculated by Aspen Plus and GAMS (errors less than ±0.6%).

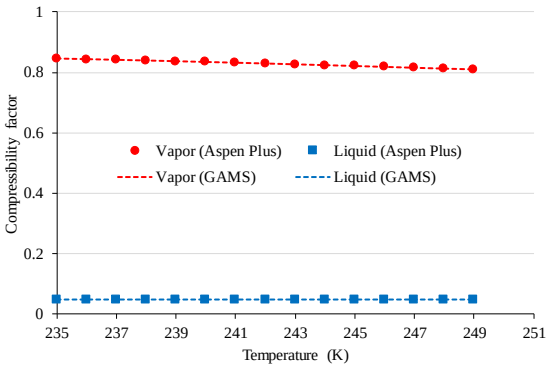

(a) Compressibility factor of vapor and liquid

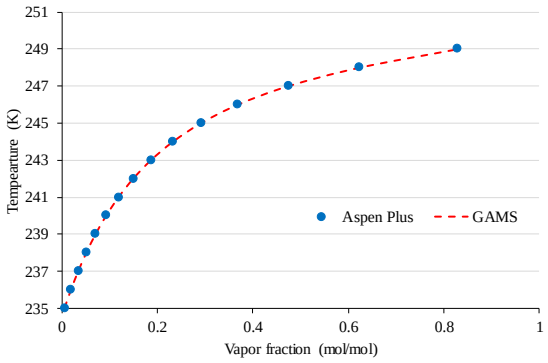

(b) Vapor fraction

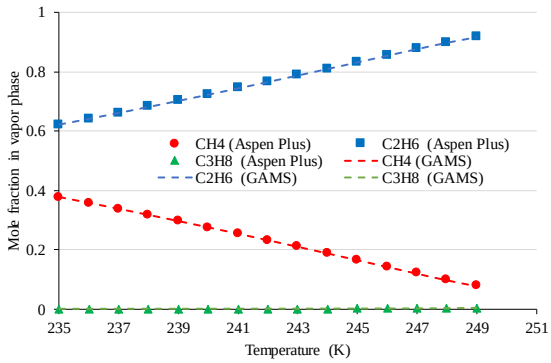

(c) Mole fraction of components

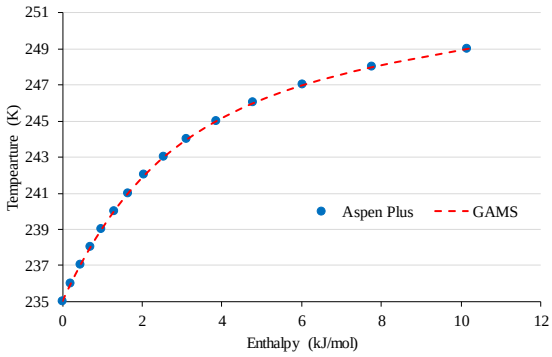

(d) Enthalpy change

Figure 2: Validation of GAMS results with Aspen Plus simulation

Table 2 presents the optimal process configuration of the process. The maximum net power output is 1.65 kW LNG, with a thermal efficiency of 15.9%. The outlet pressure of turbine is 248 kPa, at which the working fluid s_{hwfin} is a saturated vapor. The reason is that our model maximizes the net power output, and thus the working fluid tends to expand to its limit to achieve the largest work output. Moreover, the temperature at the $COND$ outlet is at 176.1 K, which is slightly higher than its dew point temperature (175.7 K). Although it is counterintuitive to subcool a working fluid as it hampers thermal efficiency of power cycle, the subcooling also lowers the pump work, resulting in a larger power output. Here the working fluid is pumped to 1375 kPa and heated up by $EVAP$ with a heat duty of 10.5 kJ/mol LNG.

Table 2 also provides the optimal composition of working fluid, which mainly consists of lighter alkanes. This is likely due to the lower dew point temperature of the mixture, which allows a larger expansion ratio without condensing into liquid. Here C_2H_6 is the major component for its relatively low boiling point while it is hot enough to regasify LNG. A small amount of CH_4 is also used to lower the dew point temperature and reduce the exergy loss as it is indicated **Figure 3**: a gradual temperature slide of the mixture (working fluid) provides a better match between the hot (the working fluid) and

cold (LNG) streams' T-H profiles at $COND$.

Figure 4 compares our optimal solution with literature results (Lee, U. and Mitsos, 2017, Liu and Guo, 2011, Sun et al., 2014, Lu and Wang, 2009) and shows a significant improvement achieved by our ORC-LNG process. For net power output, our process generates 24 % more electricity than the highest reported results. Moreover, our thermal efficiency is over 67% higher than with previous studies.

Table 2: Optimal design of the ORC-LNG process

Specifications		**Working Fluid Composition (mol/mol)**	
Power output of $TURB$ (kW)	1.41	CH_4	0.067
Power input of $PUMPWF$ (kW)	0.04	C_2H_6	0.923
Heat duty of $EVAP$ (kW)	10.6	C_3H_8	0.006
Thermal efficiency (%)	12.9	n-C_4H_{10}	0
Outlet pressure of $TURB$ (kPa)	248		
Outlet pressure of $PUMPWF$ (kPa)	1375		
Working fluid flow rate (mol/s)	0.562		

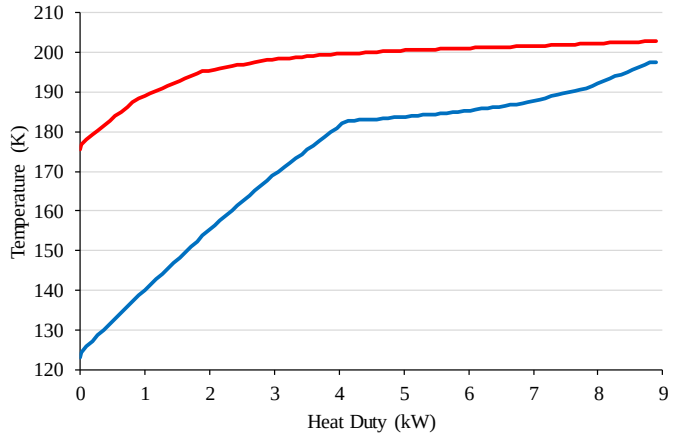

Figure 3: T-H profiles of hot and cold streams at $COND$

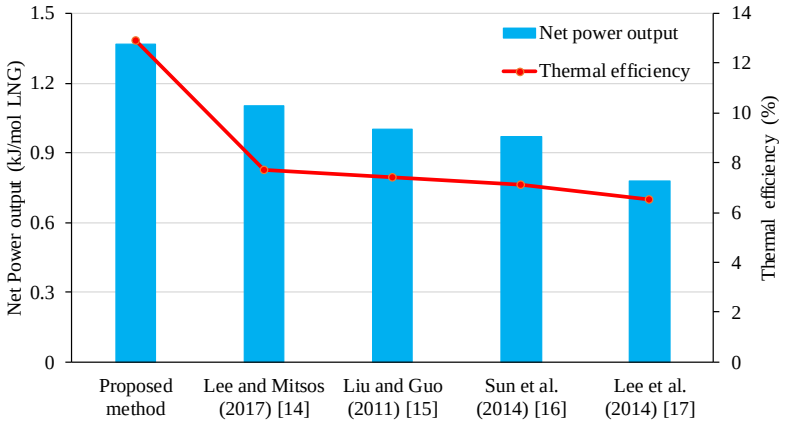

Figure 4: Comparison of the net power output and thermal efficiency with literature data

5. CONCLUSIONS

An equation-based model has been proposed for cold energy recovery of LNG regasification using ORC. Working fluid composition, process design, and heat integration of the process are jointly considered and simultaneously optimized. The proposed model has been proven to be both accurate and efficiency in its computational performance. The results have demonstrated that the equation-based model brings significant improvement in net power output and thermal efficiency to the ORC.

NOMENCLATURE

LHS	left hand side
LNG	liquefied natural gas
MINLP	mixed-integer nonlinear programming
ORC	organic Rankine cycle
RHS	right hand side
SRK	Soave-Redlich-Kwang

REFERENCES

Brooke, A., Kendrick, D., Meeraus, A. and Raman, R., 2003. *GAMS: a users guide*. Washington, DC, United States: GAMS Development Corporation.

Bussieck, M.R. and Drud, A., 2001. SBB: A new solver for mixed integer nonlinear programming. *Talk, OR*, .

Chu, S. and Majumdar, A., 2012. Opportunities and challenges for a sustainable energy future. *Nature*, **488**(7411), pp. 294.

ExxonMobil, 2018. *2018 Outlook for Energy: A View to 2040*.

Hui, C., 2014. Optimization of heat integration with variable stream data and non-linear process constraints. *Computers & Chemical Engineering*, **65**(0), pp. 81-88.

Kamath, R.S., Biegler, L.T. and Grossmann, I.E., 2010. An equation-oriented approach for handling thermodynamics based on cubic equation of state in process optimization. *Computers & Chemical Engineering*, **34**(12), pp. 2085-2096.

Kanbur, B.B., Xiang, L., Dubey, S., Choo, F.H. and Duan, F., 2017. Cold utilization systems of LNG: a review. *Renewable and sustainable energy reviews*, **79**, pp. 1171-1188.

Lee, S., 2017. Multi-parameter optimization of cold energy recovery in cascade Rankine cycle for LNG regasification using genetic algorithm. *Energy*, **118**, pp. 776-782.

Lee, U. and Mitsos, A., 2017. Optimal multicomponent working fluid of organic Rankine cycle for exergy transfer from liquefied natural gas regasification. *Energy*, **127**, pp. 489-501.

Liu, Y. and Guo, K., 2011. A novel cryogenic power cycle for LNG cold energy recovery. *Energy*, **36**(5), pp. 2828-2833.

Lu, T. and Wang, K., 2009. Analysis and optimization of a cascading power cycle with liquefied natural gas (LNG) cold energy recovery. *Applied Thermal Engineering*, **29**(8-9), pp. 1478-1484.

Luo, X., Wang, Y., Liang, J., Qi, J., Su, W., Yang, Z., Chen, J., Wang, C. and Chen, Y., 2019. Improved correlations for working fluid properties prediction and their application in performance evaluation of sub-critical Organic Rankine Cycle. *Energy*, **174**, pp. 122-137.

Park, J., Lee, I., You, F. and Moon, I., 2019. Economic process selection of LNG regasification: power generation and energy storage applications. *Industrial & Engineering Chemistry Research*, **58**(12), pp. 4946-4956.

Soave, G., 1972. Equilibrium constants from a modified Redlich-Kwong equation of state. *Chemical Engineering Science*, **27**(6), pp. 1197-1203.

Sun, H., Zhu, H., Liu, F. and Ding, H., 2014. Simulation and optimization of a novel Rankine power cycle for recovering cold energy from liquefied natural gas using a mixed working fluid. *Energy*, **70**, pp. 317-324.

U.S. Energy Information Administration, 2017. *International energy outlook 2017*. DOE/EIA-0484(2017). Washington D.C., United States of America: U.S. Energy Information Administration.

ACKNOWLEDGEMENT

The authors appreciate the financial support from the “One-Hundred Young Talents” program of Guangdong University of Technology (220413284) and Foshan Municipal Science and Technology Bureau project (2015IT100162).